Reanalysis of weak radiative decays of hyperons

R. C. Verma
Department of Physics, Panjab University, Chandigarh 160 014, India

Avinash Sharma
Department of Physics, Kurukshetra University, Kurukshetra 132 119, India

(Received 15 April 1988)

In light of recent measurements of the $\Sigma^+ \to p\gamma$ asymmetry and the branching ratio of $\Xi^- \to \Sigma^-\gamma$ decay, we reinvestigate the single-quark- and two-quark-transition contributions to the weak radiative decays of hyperons. We find that a small contribution from single-quark transition, necessary for $\Xi^- \to \Sigma^-\gamma$ decay, enhances the $\Sigma^+ \to p\gamma$ decay asymmetry to around -0.59.

I. INTRODUCTION

Radiative weak decays have attracted the attention of theorists for a long time as these can probe the structure of weak nonleptonic interactions. Theoretically, these decays present fewer complications due to the strong-interaction interference than do the weak nonleptonic decays. On the other hand, progress on the experimental side has been very slow because of their low branching ratios. However, recently the decay parameters of $\Xi^- \to \Sigma^-\gamma$ and $\Sigma^+ \to p\gamma$ have been measured[1–5] more accurately, warranting a detailed reanalysis of these decays.

In earlier theoretical attempts,[6] a combination of pole-model framework and internal symmetries have been used. Although, these attempts reproduced the decay rates of the right order of magnitude, the observed large negative asymmetry of $\Sigma^+ \to p\gamma$ process (hereafter referred to as α_{Σ^+}) has long been a standing problem. With the advent of electroweak gauge theory, it has become desirable to investigate these decays in the framework of quark models. At the quark level, three types of processes, i.e., single-, two-, and three-quark transitions, can contribute to the radiative weak decays. A pioneering attempt in this direction was made by Gilman and Wise[7] who assumed the dominance of single-quark transition $s \to d\gamma$. They obtained a rather small positive asymmetry α_{Σ^+}. Later, QCD corrections[8,9] and long-distance effects[10] have been considered for the single-quark processes. Though such effects tend to enhance its contribution, it has been noted[7–11] that the single-quark transition alone is inadequate in describing these decays. Contributions from the two- and three-quark transitions have also been investigated.[12–16] The three-quark transitions have been shown to be negligible, whereas the two-quark transitions reproduce the available data to a reasonable extent. The two-quark process $s+u \to u+d+\gamma$, which proceeds via W exchange, appears to be dominant in the decays under consideration. This predicts α_{Σ^+} to be -0.30, i.e., of the right sign though small in magnitude. However, the W-exchange transition does not contribute to $\Xi^- \to \Sigma^-\gamma$ and $\Omega^- \to \Xi^-\gamma$, as the initial baryon does not contain a valence u quark. Therefore, the measurement of decay widths and asymmetries of these decays are of particular importance in deciding the relative strength of the single- and two-quark transitions. With this motivation we reanalyze the radiative weak decays of hyperons within the constituent-quark-model framework.

In Secs. II and III we describe the two- and single-quark Hamiltonians, respectively. Section IV deals with the extraction of the decay amplitudes. Numerical results are computed and discussed in the last section.

II. TWO-QUARK W-EXCHANGE HAMILTONIAN

We evaluate the effective electroweak Hamiltonian for the process $s+u \to u+d+\gamma$. Various W-exchange diagrams contributing to this process are shown in Figs. 1 and 2. If the photon involved were soft, one could expect the weak bremsstrahlung amplitude to diverge as $1/k$. As the photon emitted is far from being soft (~ 100–200 MeV), we have carried out an expansion of the amplitude in k such that each stage respects gauge invariance. We work in the Coulomb gauge: ϵ_0 and $\boldsymbol{\epsilon}\cdot\mathbf{k}=0$. The Hamiltonian for the process

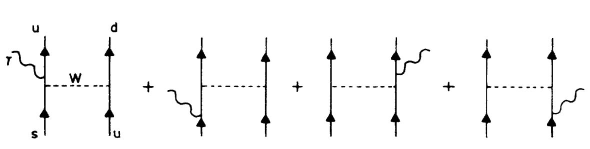

FIG. 1. Quark-quark bremsstrahlung diagrams.

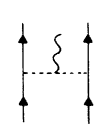

FIG. 2. An internal radiation diagram.

$$s(p_1)+u(p_2)\to u(p_3)+d(p_4)+\gamma(k) \quad (1)$$

shown in Fig. 1(a) is written as

$$\frac{e_u G_F \sin\theta_C \cos\theta_C}{\sqrt{2}2k\cdot p_3}\bar{u}(2\epsilon\cdot p_3+\epsilon\!\!/ k\!\!\!/)\gamma_\mu(1-\gamma_5)s \times \bar{d}\gamma^\mu(1-\gamma_5)u \ . \quad (2)$$

All the external quarks are assumed to be on their mass shells. In the soft-photon limit the terms proportional to $\epsilon\cdot p_3/k\cdot p_3$ diverge like $1/k$. In fact, these terms do not contribute to the decays. Summing over all the permutations for photon emission (Fig. 1) we carry out a nonrelativistic reduction. The effective Hamiltonian thus obtained is

$$H_w^{\rm PC}(\lambda_\gamma=+1)=\frac{eG_F\sin\theta_C\cos\theta_C}{(2)^{1/2}m_u}\left[\left[-\frac{k_0}{2m_u}u^\dagger\sigma_3 s\, d^\dagger\sigma_- u+u^\dagger s\, d^\dagger\sigma_- u\right]+\left[-1+\frac{k_0}{2m_u}\right]\zeta(u^\dagger\sigma_3 s\, d^\dagger\sigma_- u+u^\dagger s\, d^\dagger\sigma_- u)+\left[1+\frac{k_0}{2m_u}\right][\zeta u^\dagger\sigma_- s\, d^\dagger\sigma_3 u+(-1+\zeta)u^\dagger\sigma_- s\, d^\dagger u]\right], \quad (3a)$$

$$H_w^{\rm PV}(\lambda_\gamma=+1)=\frac{eG_F\sin\theta_C\cos\theta_C}{(2)^{1/2}m_u}\left[\left[u^\dagger\sigma_3 s\, d^\dagger\sigma_- u-\frac{k_0}{2m_u}u^\dagger s\, d^\dagger\sigma_- u\right]+\left[-1+\frac{k_0}{2m_u}\right]\zeta(u^\dagger\sigma_3 s\, d^\dagger\sigma_- u+u^\dagger s\, d^\dagger\sigma_- u)+\left[1+\frac{k_0}{2m_u}\right][(-1+\zeta)u^\dagger\sigma_- s\, d^\dagger\sigma_3 u+\zeta u^\dagger\sigma_- s\, d^\dagger u]\right], \quad (3b)$$

where $6\zeta=1-m_u/m_s$ and λ_γ is the helicity state of the photon. Terms like $O(\zeta^2)$ and $O(k^2)$ are dropped. The contribution of the internal radiative process involving two quarks (Fig. 2) is suppressed[15] by a factor $m_u k/m_W^2$ as compared to the bremsstrahlung process.

The three-quark process (Fig. 3) contributing to the weak radiative decays may also involve W exchange. This contributes mainly to the parity-conserving mode and is further suppressed due to very small probability of finding three quarks in adequate kinematic matching with the baryon.[13–15]

The decay amplitudes are evaluated by sandwiching the Hamiltonian [Eq. (3)] between the baryon wave functions, with one of the quarks as a spectator. The amplitudes thus obtained are given in Table I.

With the dominance of the two-quark W-exchange diagrams, the α_{Σ^+} has been predicted[16] to be -0.30, which is small in magnitude but is of the right sign. This happens due to the fact that the weak Hamiltonian [Eq. (3)] contains a piece which does not respect Hara's theorem as has been demonstrated by Kamal and Riazuddin.[15] The branching ratios thus calculated (column 2 of Table

TABLE I. Two-quark decay amplitudes in units of $(eG_F\sin\theta_C\cos\theta_C/\sqrt{2}m_u)\,|\psi(k)|^2$, $X=k/2m_u$ and $6\xi=(1-m_u/m_s)$.

Decay	Parity conserving (PC)	Parity violating (PV)
$\Sigma^+\to p\gamma$	$\frac{2}{9}[X+\zeta(3+X)]$	$\frac{2}{9}[-3-2X+\zeta(3+X)]$
$\Sigma^0\to n\gamma$	$\frac{1}{9\sqrt{2}}[6+2X+\zeta(-6+2X)]$	$\frac{1}{9\sqrt{2}}[-4X+\zeta(-6+2X)]$
$\Lambda\to n\gamma$	$\frac{1}{3\sqrt{6}}[2-2X+\zeta(-6+2X)]$	$\frac{1}{3\sqrt{6}}[4+\zeta(-6+2X)]$
$\Xi^0\to\Lambda\gamma$	$\frac{1}{3\sqrt{6}}(2-4\zeta)$	$\frac{1}{3\sqrt{6}}(2-4\zeta)$
$\Xi^0\to\Sigma^0\gamma$	$\frac{1}{9\sqrt{2}}(6+8X-4X\zeta)$	$\frac{1}{9\sqrt{2}}(-6-4X-4X\zeta)$
$\Xi^-\to\Sigma^-\gamma$	0	0
$\Omega^-\to\Xi^-\gamma$	0	0

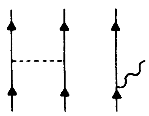

FIG. 3. Three-quark transition.

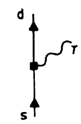

FIG. 5. Black-box diagram for single-quark transition.

III below) are consistent for the allowed decays. It is clear that the decays of Ξ^- and Ω^- hyperons cannot proceed via W-exchange diagrams and require a single-quark transition Hamiltonian which is described in the next section.

III. SINGLE-QUARK TRANSITION HAMILTONIAN

The single-quark transition, where the other two quarks of the baryon act as spectators, is generally expressed[7] in terms of two parameters a and b as follows:

$$H_{1q}=\frac{eG_F\sin\theta_C\cos\theta_C}{\sqrt{2}}\bar{d}(a+b\gamma_5)i\not{k}\not{\epsilon}s \ . \tag{4}$$

In the nonrelativistic limit, it leads to an effective Hamiltonian

$$H^{1q}_{\rm eff}=\frac{eG_F\sin\theta_C\cos\theta_C}{\sqrt{2}}kd^\dagger[ia(\boldsymbol{\epsilon}\times\hat{\mathbf{k}})\cdot\boldsymbol{\sigma}-b(\boldsymbol{\epsilon}\cdot\boldsymbol{\sigma})]s \ . \tag{5}$$

The determination of the parameters a and b depends upon the approach used to study these decays. In the following, we discuss the three major approaches.

A. Case (i): Electroweak gauge theory

The characteristics of the single-quark transition $s\to d\gamma$ in the Glashow-Weinberg-Salam model can be computed as the sum of the four diagrams shown in Fig. 4. The general calculations of the effective $s\to d\gamma$ vertex have been carried out by Deshpande and Eilam[17] and they obtained

$$a=A(m_d+m_s)\ ,\quad b/a=(m_s-m_d)/(m_s+m_d)\simeq\tfrac{1}{4}\ .$$

The Glashow-Iliopoulos-Maiani (GIM) cancellation[17–19] reduces the scale parameter A significantly. For a typical top-quark-mass value $m_t\simeq 30$ GeV, A comes out to be $\sim -6.3\times10^{-5}$, which suppresses[14] the single-quark transitions by many orders of magnitudes in comparison with the two-quark transitions.

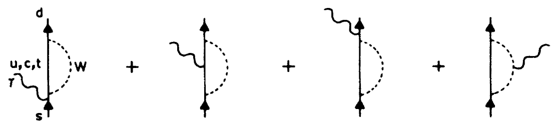

FIG. 4. Single-quark diagrams in electroweak gauge theory.

B. Case (ii): QCD effects

Gluonic corrections have also been considered on the processes shown in Fig. 4. It has been shown[8] that in two-loop graphs of W and the gluon, the GIM cancellation factors get replaced by quark-mass ratios which results in an enhancement (although not sufficient) of the scale parameter A by 2 orders of magnitude. The QCD-renormalized effective weak Hamiltonian, then fixes

$$b/a=+1\ .$$

It may be mentioned that the gluons may also affect the two-quark processes. Lo-Chong[13] has studied one-loop QCD corrections to the two-quark W-exchange diagrams. These, however, have practically no effect on the numerics of the radiative weak decays.[20]

C. Case (iii): Long-distance effects

The QCD short-distance enhanced $s\to d\gamma$ vertex is not sufficient as it yields $B(\Xi^-\to\Sigma^-\gamma)\simeq1.8\times10^{-5}$ (Ref. 8), which still is an order of magnitude smaller than the recently measured[1] value $(2.27\pm1.02)\times10^{-4}$. It has been argued[10,11] that the long-distance part of the effective electroweak interaction may be of greater importance than the short-distance part. Using the chiral-Lagrangian approach, Palle[10] has recently studied long-distance effects to $s\to d\gamma$ induced radiative weak decays. The decay rates thus obtained remain 2 orders of magnitude smaller than the one evaluated for the W-exchange two-quark transition. However, the α_{Σ^+} does acquire a large negative value (-0.50) in contrast with the short-distance results. Translating it in terms of the parameters a and b, it effectively corresponds to

TABLE II. Single-quark decay amplitudes in units of $(eG_F\sin\theta_C\cos\theta_C/\sqrt{2})kF(k)$.

Decay	PC	PV
$\Sigma^+\to p\gamma$	$-\frac{1}{3}a$	$-\frac{1}{3}b$
$\Sigma^0\to n\gamma$	$\frac{1}{3\sqrt{2}}a$	$\frac{1}{3\sqrt{2}}b$
$\Lambda\to n\gamma$	$\frac{3}{\sqrt{6}}a$	$\frac{3}{\sqrt{6}}b$
$\Xi^0\to\Lambda\gamma$	$\frac{1}{\sqrt{6}}a$	$\frac{1}{\sqrt{6}}b$
$\Xi^0\to\Sigma^0\gamma$	$-\frac{5}{3\sqrt{2}}a$	$-\frac{5}{3\sqrt{2}}b$
$\Xi^-\to\Sigma^-\gamma$	$\frac{5}{3}a$	$\frac{5}{3}b$
$\Omega^-\to\Xi^-\gamma$	$\frac{\sqrt{6}}{3}a$	$\frac{\sqrt{6}}{3}b$

TABLE III. Branching ratios in units of 10^{-3}.

Decays	Pure two-quark transitions ($b=a=0$)	Electroweak gauge theory ($b/a \approx \frac{1}{4}$)	QCD effects ($b/a \approx +1$)	Long-distance effects ($b/a \approx -\frac{1}{4}$)	Experimental	Ref.
$\Gamma(\Sigma^+ \to p\gamma)/\Gamma(\Sigma^+ \to p\pi^0)$	2.32	2.32	1.95	2.65	$2.46^{+0.30}_{-0.35}$	2
$\Gamma(\Lambda \to n\gamma)/\Gamma(\Lambda \to n\pi^0)$	3.58	2.67	1.00	4.64	2.85 ± 1.0	24
$\Gamma(\Xi^0 \to \Lambda\gamma)/\Gamma(\Xi^0 \to \Lambda\pi^0)$	0.70	0.36	0.29	0.57	1.3 ± 0.2	25
$\Gamma(\Xi^0 \to \Sigma^0\gamma)/\Gamma(\Xi^0 \to \Lambda\pi^0)$	2.62	4.43	4.58	4.06	<70	23
$\Gamma(\Xi^- \to \Sigma^-\gamma)/\Gamma(\Xi^- \to \Lambda\pi^-)$	0	0.23	0.23	0.23	0.227 ± 0.102[a]	1
$\Gamma(\Omega^- \to \Xi^-\gamma)/\Gamma(\Omega^- \to \text{all})$	0	0.52	0.52	0.52	<2.2	23

[a]Input.

$$b/a \simeq -\tfrac{1}{4} .$$

Looking at the uncertainties in the determination of a and b, we perform a general "black-box" treatment[7] (Fig. 5) of the $s \to d\gamma$ vertex which includes all possible cases. The single-quark decay amplitudes thus obtained are presented in Table II.

IV. DETERMINATION OF DECAY RATES AND ASYMMETRIES

The gauge-invariant form of the radiative weak decay amplitude $B_i \to B_f \gamma$ is written as

$$H_w = \frac{eG_F \sin\theta_C \cos\theta_C}{\sqrt{2}} \bar{B}_f (F_1 + F_2\gamma_5) \not{k} \not{\epsilon} B_i \ , \tag{6}$$

where B_i and B_f denote the Dirac spinors for initial and final baryons, respectively. The decay rates are then given by

$$\Gamma(B_i \to B_f \gamma) = \frac{e^2 G_F{}^2 \sin^2\theta_C \cos^2\theta_C}{2\pi} (|F_1|^2 + |F_2|^2) k^3 \tag{7}$$

and the asymmetry is

$$\alpha(B_i \to B_f \gamma) = \frac{2\,\mathrm{Re}(F_1 F_2^*)}{|F_1|^2 + |F_2|^2} \ . \tag{8}$$

The baryon decay amplitudes are extracted in the spirit of the works of Kamal and Verma[12] and Eckert and Morel[14] by adding the contributions from single- and two-quark processes. The appropriate scale factors required are obtained as follows.

A baryon B_i is taken to split into three valence quarks which in turn interact and then give rise to the final baryon state after emitting the photon. The requirement that the quarks should have kinematic matching with the baryons introduces in the decay amplitudes a dimensionless factor $F(k)$ for the single-quark transitions and a factor $|\psi(k)|^2$, having dimensions (energy)^3, for the two-quark transitions. The factor $F(k)$ which depends upon the initial- and final-state wave functions is normalized so that $F(0)=1$ in the constituent-quark model. It is assumed[7] that $F(k)$ does not depend on photon momentum (k) significantly. This is justified in view of the successful predictions of $\Delta^+ \to p\gamma$ and $\Sigma^0 \to \Lambda\gamma$ decays in the constituent-quark-model framework. However, it may be remarked that the magnitude of $F(k)$ is not needed for the present calculations as it gets absorbed into the free parameters a and b. The other factor $|\psi(k)|^2$, which also appears in the analysis of weak nonleptonic decays, varies very slowly[14,21,22] with k and lies in the range 10^{-3}–10^{-2} GeV^3.

V. NUMERICAL RESULTS AND DISCUSSIONS

We combine the single- and two-quark transition amplitudes as discussed in the last section. In view of the uncertain state in determination of the single-quark transition parameters a and b, we present the results for all three cases discussed in Sec. III, by having $b/a \approx \frac{1}{4}, 1, -\frac{1}{4}$. The parity-conserving parameter a is fixed from the recently observed branching ratio[1]

TABLE IV. Decay asymmetries.

Decays	Pure two-quark transitions ($b=a=0$)	Electroweak gauge theory ($b/a \approx \frac{1}{4}$)	QCD effects ($b/a \approx +1$)	Long-distance effects ($b/a \approx -\frac{1}{4}$)	Experimental	Ref.
$\Sigma^+ \to p\gamma$	-0.30	-0.59	-0.56	-0.55	-0.72 ± 0.29	23
$\Lambda \to n\gamma$	0.58	-0.66	-0.51	-0.52		
$\Xi^0 \to \Lambda\gamma$	1.00	0.87	1.00	0.74		
$\Xi^0 \to \Sigma^0\gamma$	0.96	0.90	0.97	0.81		
$\Xi^- \to \Sigma^-\gamma$	0	0.44	1.00	-0.44		
$\Omega^- \to \Xi^-\gamma$	0	0.44	1.00	-0.44		

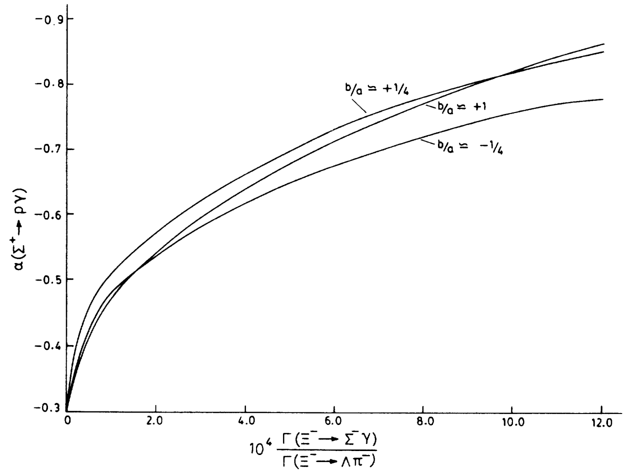

FIG. 6. Variation of α_{Σ^+} vs $B(\Xi^-\to\Sigma^-\gamma)$.

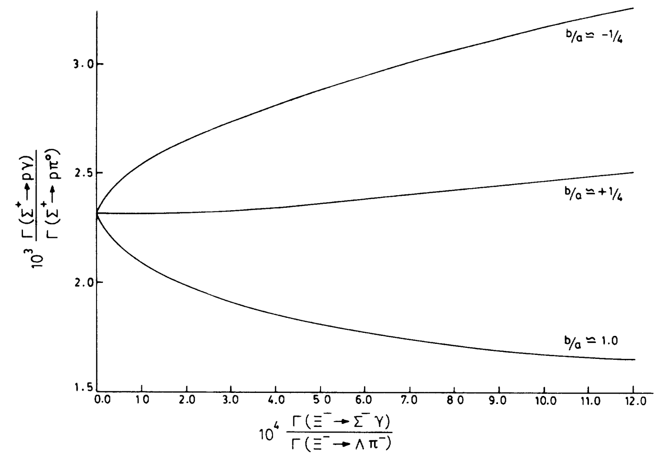

FIG. 7. Variation of $B(\Sigma^+\to p\gamma)$ with $B(\Xi^-\to\Sigma^-\gamma)$.

$$\Gamma(\Xi^-\to\Sigma^-\gamma)/\Gamma(\Xi^-\to\Lambda\pi^-)=(2.27\pm1.02)\times10^{-4}\ .$$

It lies within $(-3$ to $-5)\times10^{-3}$ GeV for these cases implying thereby that the strong-interaction effects on the $s\to d\gamma$ vertex are significant. Furthermore, the scale factor $|\psi(k)|^2\simeq|\psi(0)|^2\simeq10^{-3}$ GeV^3 and the quark-mass values $m_u\simeq m_d\simeq0.336$ GeV, $m_s\simeq0.540$ GeV are used. The branching ratios and asymmetries thus obtained are presented in Tables III and IV, respectively. Though, the branching ratios are by and large consistent with the available data for all the cases, it is evident that the short-distance QCD effects are a bit insufficient in reproducing the available data; and the long-distance effects seem to be necessary. It is also noticed that in the presence of the single-quark transition, α_{Σ^+} gets doubled to $\simeq-0.59$ as compared to the one obtained with the pure two-quark transitions. As the α_{Σ^+} comes out to be nearly equal for all the cases, observation of the other decay asymmetries, particularly of $\Xi^-\to\Sigma^-\gamma$, is needed in order to distinguish them. It may be noticed that the $\Lambda\to n\gamma$ decay asymmetry becomes negative in the presence of the single-quark transitions.

Since the branching ratio $B(\Xi^-\to\Sigma^-\gamma)$ is measured for the first time, we also investigate the variation of $\Sigma^+\to p\gamma$ decay parameters with respect to $B(\Xi^-\to\Sigma^-\gamma)$ and obtain

$$\frac{\Gamma(\Sigma^+\to p\gamma)}{\Gamma(\Sigma^+\to p\pi^0)}\simeq2.32\times10^{-3}\left[1+0.01B_{\Xi^-}-0.21\left[\frac{p-0.16}{(1+p^2)^{1/2}}\right]\sqrt{B_{\Xi^-}}\right]$$

and

$$\alpha(\Sigma^+\to p\gamma)\simeq-0.30\left[1-0.03B_{\Xi^-}+0.65\left[\frac{1+0.16p}{(1+p^2)^{1/2}}\right]\sqrt{B_{\Xi^-}}\right]\ ,$$

where $p\equiv b/a$ and

$$B_{\Xi^-}=10^4\times\frac{\Gamma(\Xi^-\to\Sigma^-\gamma)}{\Gamma(\Xi^-\to\Lambda\pi^-)}\ .$$

$B(\Xi^-\to\Sigma^-\gamma)$ is varied from zero to the earlier upper limit 1.2×10^{-3} (Ref. 23). The relevant variations are shown in Figs. 6 and 7. It is noticed that the $B(\Sigma^+\to p\gamma)$ is rather less sensitive to $B(\Xi^-\to\Sigma^-\gamma)$ whereas the $\alpha(\Sigma^+\to p\gamma)$ shows an increasing trend with increasing $B(\Xi^-\to\Sigma^-\gamma)$.

ACKNOWLEDGMENT

The authors are thankful to Professor M. P. Khanna for reading the manuscript.

[1]S. F. Biagi *et al.*, Z. Phys. C **35**, 143 (1987).
[2]M. Bourquin, in *Proceedings of the XXIII International Conference on High Energy Physics*, Berkeley, California, 1986, edited by S. C. Loken (World Scientific, Singapore, 1987), p. 880.
[3]S. F. Biagi *et al.*, Z. Phys. C **28**, 495 (1985).
[4]M. Kobayashi *et al.*, Phys. Rev. Lett. **59**, 868 (1987).
[5]A. Manz *et al.*, Phys. Lett. **96B**, 217 (1980).
[6]P. N. Pandit, R. C. Verma, and M. P. Khanna, Prog. Theor.

Phys. **64**, 2158 (1980); F. E. Close and H. R. Rubinstein, Nucl. Phys. **B173**, 477 (1980); I. Picek, Phys. Rev. D **21**, 3169 (1980); K. G. Rauh, Z. Phys. C **10**, 81 (1981); M. B. Gavela *et al.*, Phys. Lett. **101B**, 417 (1981); M. A. Shifman, A. I. Vainshtein, and W. I. Zakharov, Yad. Fiz. **34**, 1392 (1981) [Sov. J. Nucl. Phys. **34**, 773 (1981)]; S. N. Biswas, A. Goyal, and J. N. Passi, Phys. Rev. D **25**, 2356 (1982); E. Golowich and B. R. Holstein, *ibid.* **26**, 182 (1982); M. D. Scadron and M. Visinecu, *ibid.* **28**, 1117 (1983); R. Safadi and P. Singer, *ibid.* **37**, 697 (1988). A more comprehensive list of works done before 1980 is given in Ref. 5.

[7]F. J. Gilman and M. B. Wise, Phys. Rev. D **19**, 976 (1979).

[8]L. Bergström and P. Singer, Phys. Lett. **169B**, 297 (1986).

[9]M. K. Gaillard, X. Q. Li, and S. Rudaz. Phys. Lett. **158B**, 158 (1985).

[10]D. Palle, Phys. Rev. D **36**, 2863 (1987).

[11]Ya. I. Kagon and M. A. Shifman, Yad. Fiz. **38**, 1045 (1983) [Sov. J. Nucl. Phys. **38**, 628 (1983)].

[12]A. N. Kamal and R. C. Verma, Phys. Rev. D **26**, 190 (1982).

[13]Lo-Chong Hua, Phys. Rev. D **26**, 199 (1982).

[14]P. Eckert and B. Morel, Universite de Geneve Report No. UGVA-DPT 1982/03-340 (unpublished).

[15]A. N. Kamal and Riazuddin, Phys. Rev. D **28**, 2317 (1983).

[16]R. C. Verma and A. Sharma, J. Phys. G **12**, 1329 (1986).

[17]N. G. Deshpande and G. Eilam, Phys. Rev. D **26**, 2463 (1982); T. Inami and C. S. Lim, Prog. Theor. Phys. **65**, 297 (1981); N. G. Deshpande, G. Eilam, and W. L. Spence, Phys. Lett. **108B**, 42 (1982).

[18]B. W. Lee and M. K. Gaillard, Phys. Rev. D **10**, 897 (1974); S. P. Chia and G. Rajgopal, Phys. Lett. **156B**, 405 (1985).

[19]J. O. Eeg, Z. Phys. C **21**, 253 (1984); S. G. Kamath, Nucl. Phys. **B198**, 61 (1982).

[20]In addition, the penguin diagram may also contribute to $\Xi^- \to \Sigma^- \gamma$ and similar decays, which however has been found (Ref. 19) to be even smaller than the single-quark transition. In the nonleptonic decays also, contrary to the early hopes, the penguin diagrams are probably not responsible for $\Delta I = \frac{1}{2}$ dominance [H.Y. Cheng, Indiana University Report No. 132, 1987 (unpublished)].

[21]Riazuddin and Fayyazuddin, Phys. Rev. D **18**, 1578 (1978); **19**, 1630(E) (1979).

[22]A. De Rújula, H. Georgi, and S. L. Glashow, Phys. Rev. D **12**, 147 (1975).

[23]Particle Data Group, M. Aguilar-Benitez *et al.*, Phys. Lett. **170B**, 17 (1986).

[24]S. F. Biagi *et al.*, Z. Phys. C **30**, 201 (1986).

[25]C. James *et al.*, in *Proceedings of XXIII International Conference on High Energy Physics* (Ref. 2), p. 877.